Science Advances

AAAS

advances.sciencemag.org/cgi/content/full/3/11/e1700537/DC1

Supplementary Materials for

Should coastal planners have concern over where land ice is melting?

Eric Larour, Erik R. Ivins, Surendra Adhikari

Published 15 November 2017, *Sci. Adv.* **3**, e1700537 (2017)
DOI: 10.1126/sciadv.1700537

This PDF file includes:

Supplementary Materials

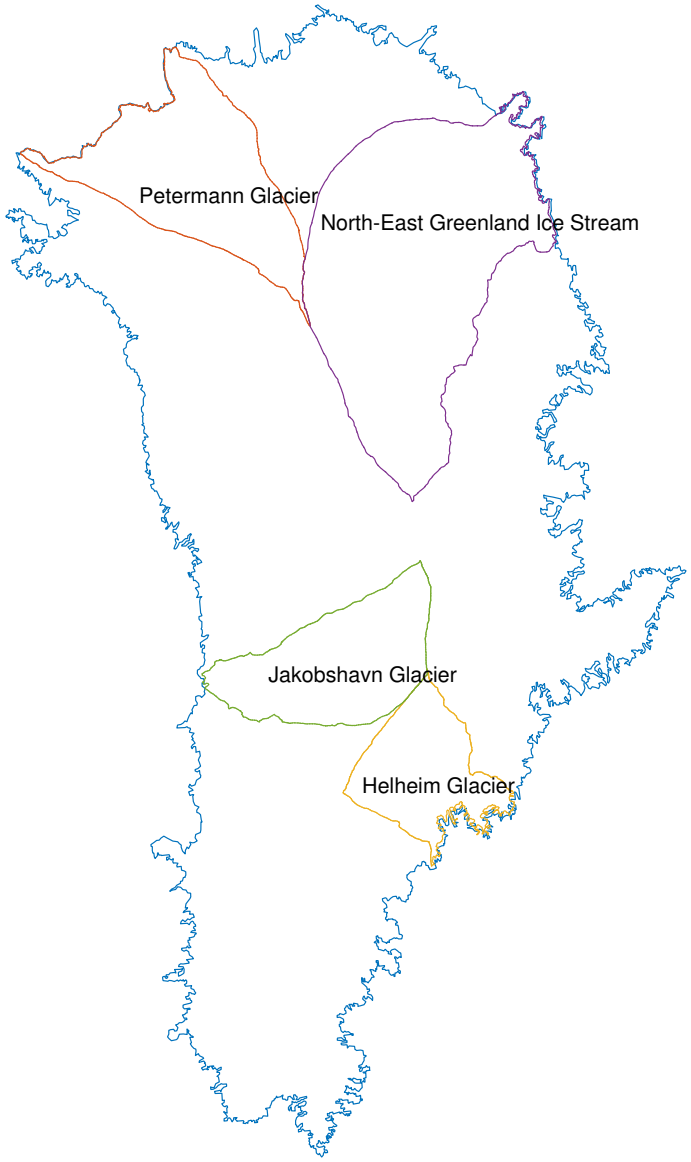

fig. S1. Greenland basins used in Table 1. Contours for the four Greenland basins (Petermann Glacier, North-East Greenland Ice Stream, Jakobsvhavn Glacier and Helheim Glacier) used in Table 1. The overall contour of Greenland is also provided for reference.

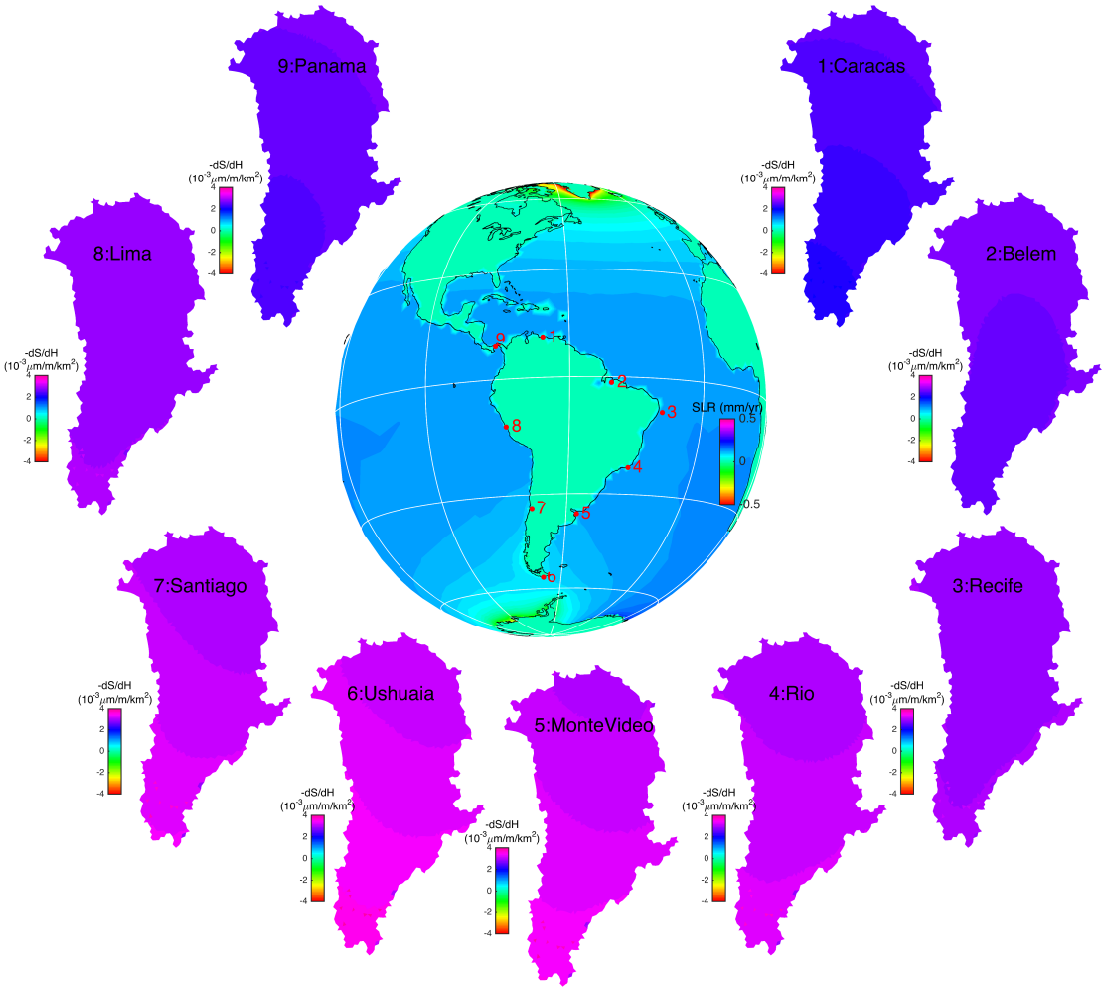

fig. S2. Sensitivity of SLR along the South American coastline to GrIS thickness variations. Gradient −dS/dH (in μm/m/km^2) at select South-American coastal cities. Maps 1 through 9 correspond, respectively, to gradients computed for each of the named ports numbered clockwise from Caracas. See Fig. 2 caption for a detailed explanation of how the forward run and its gradient were computed.

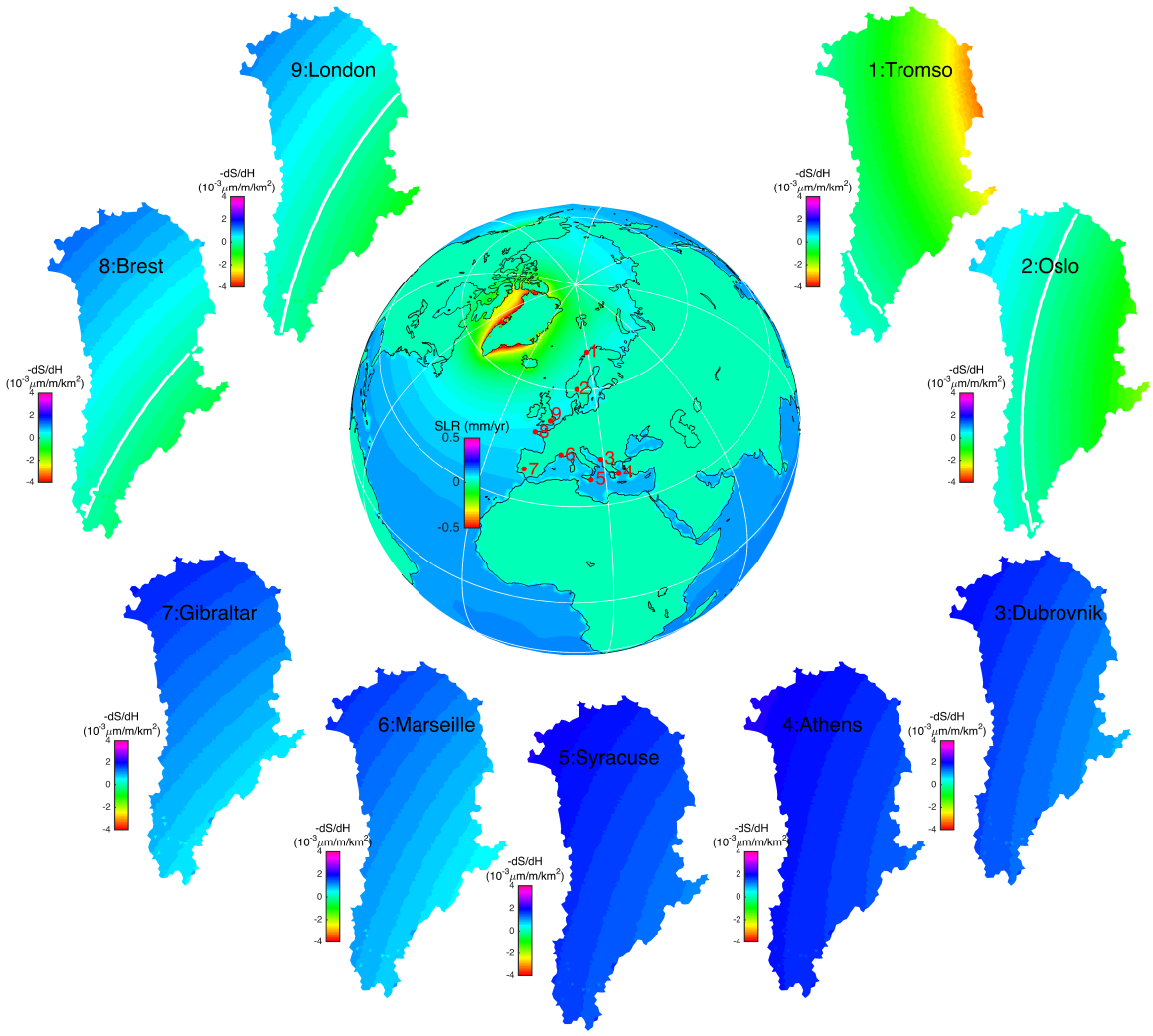

fig. S3. Sensitivity of SLR along the European coastline to GrIS thickness variations. Gradient −dS/dH (in μm/m/km^2) at select European coastal cities. Maps 1 through 9 correspond, respectively, to gradients computed for each of the named ports numbered clockwise from Tromso. The zero level for the gradient is marked by a white line. See Fig. 2 caption for a detailed explanation of how the forward run and its gradient were computed.

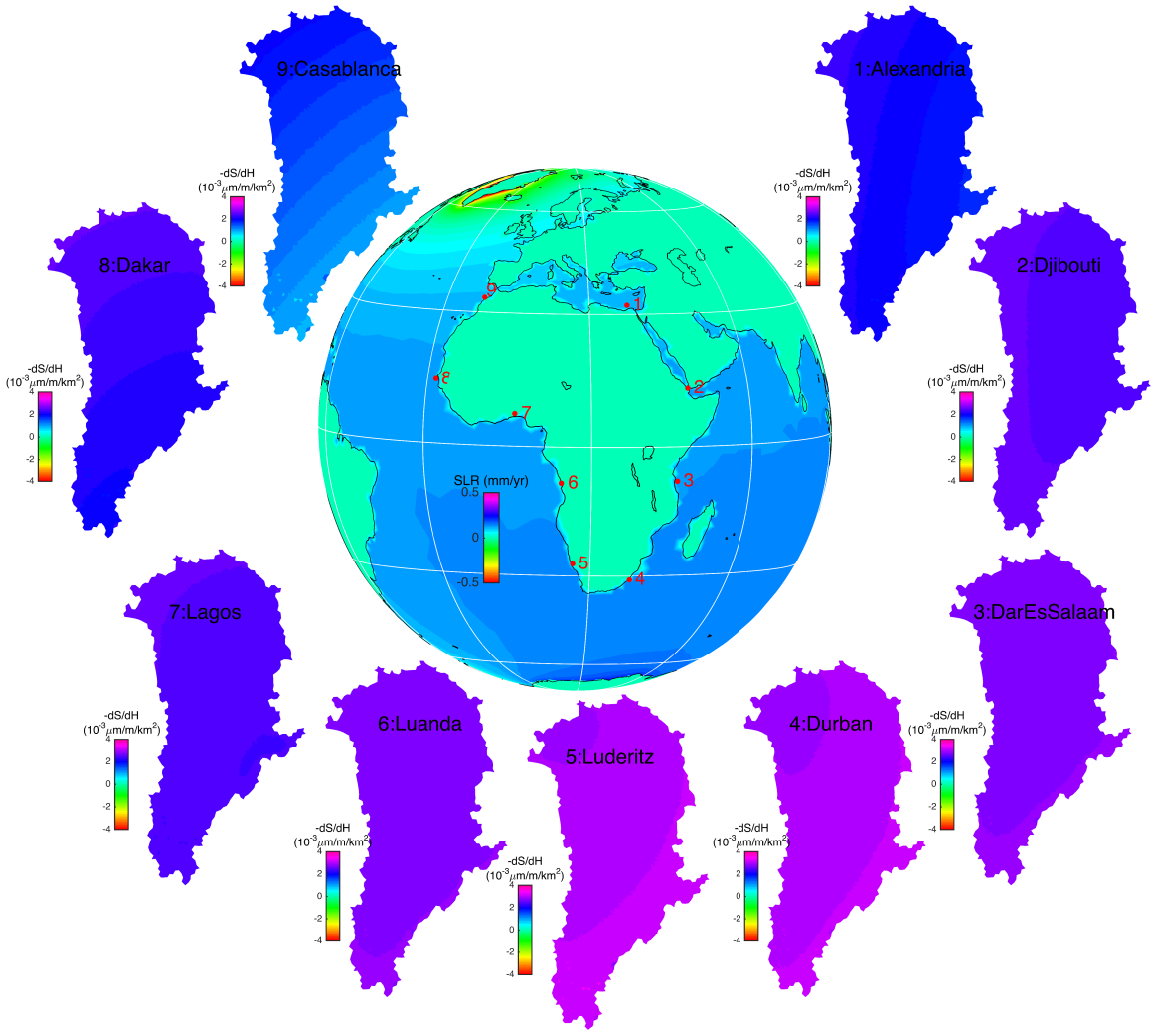

fig. S4. Sensitivity of SLR along the African coastline to GrIS thickness. Gradient −dS/dH (in μm/m/km^2) at select African coastal cities. Maps 1 through 9 correspond, respectively, to gradients computed for each of the named ports numbered clockwise from Alexandria. See Fig. 2 caption for a detailed explanation of how the forward run and its gradient were computed.

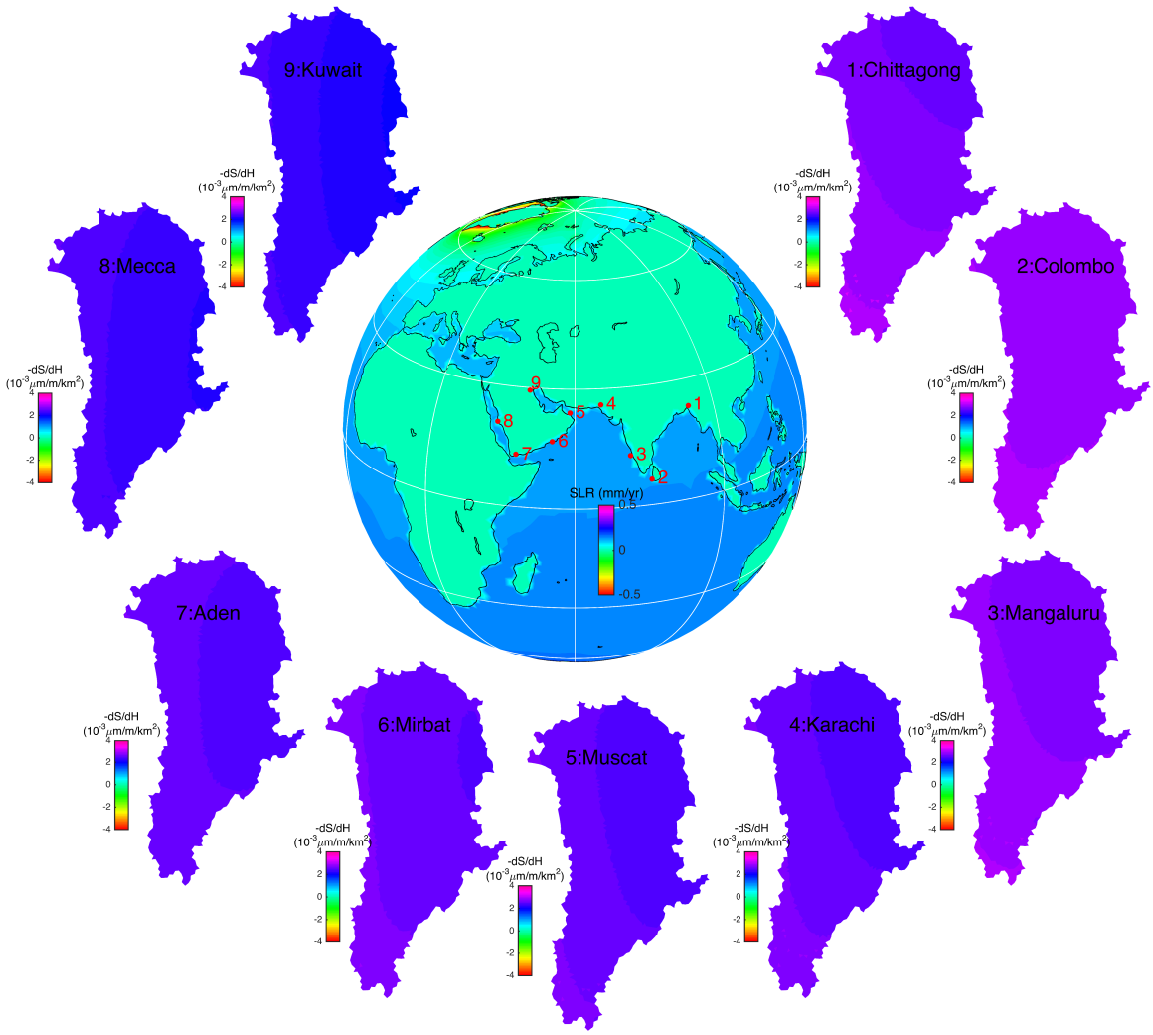

fig. S5. Sensitivity of SLR along the Middle East and South Asian coastlines to GrIS thickness variations. Gradient −dS/dH (in μm/m/km^2) at select Middle-East and South-Asian coastal cities. Maps 1 through 9 correspond, respectively, to gradients computed for each of the named ports numbered clockwise from Chittagong. See Fig. 2 caption for a detailed explanation of how the forward run and its gradient were computed.

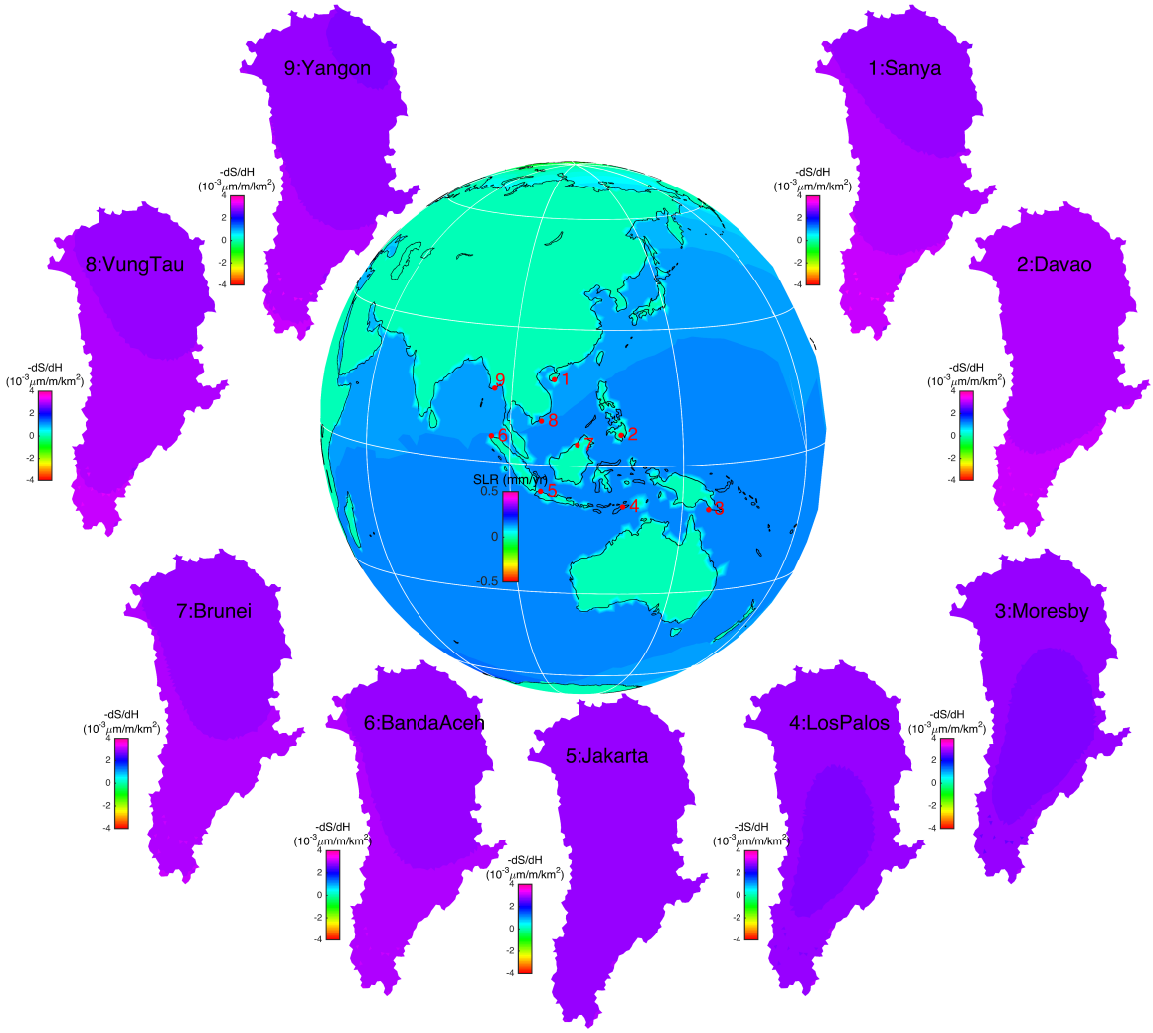

fig. S6. Sensitivity of SLR along the Southeast Asian coastline to GrIS thickness variations. Gradient −dS/dH (in μm/m/km2) at select South-East Asian coastal cities. Maps 1 through 9 correspond, respectively, to gradients computed for each of the named ports numbered clockwise from Sanya. See Fig. 2 caption for a detailed explanation of how the forward run and its gradient were computed.

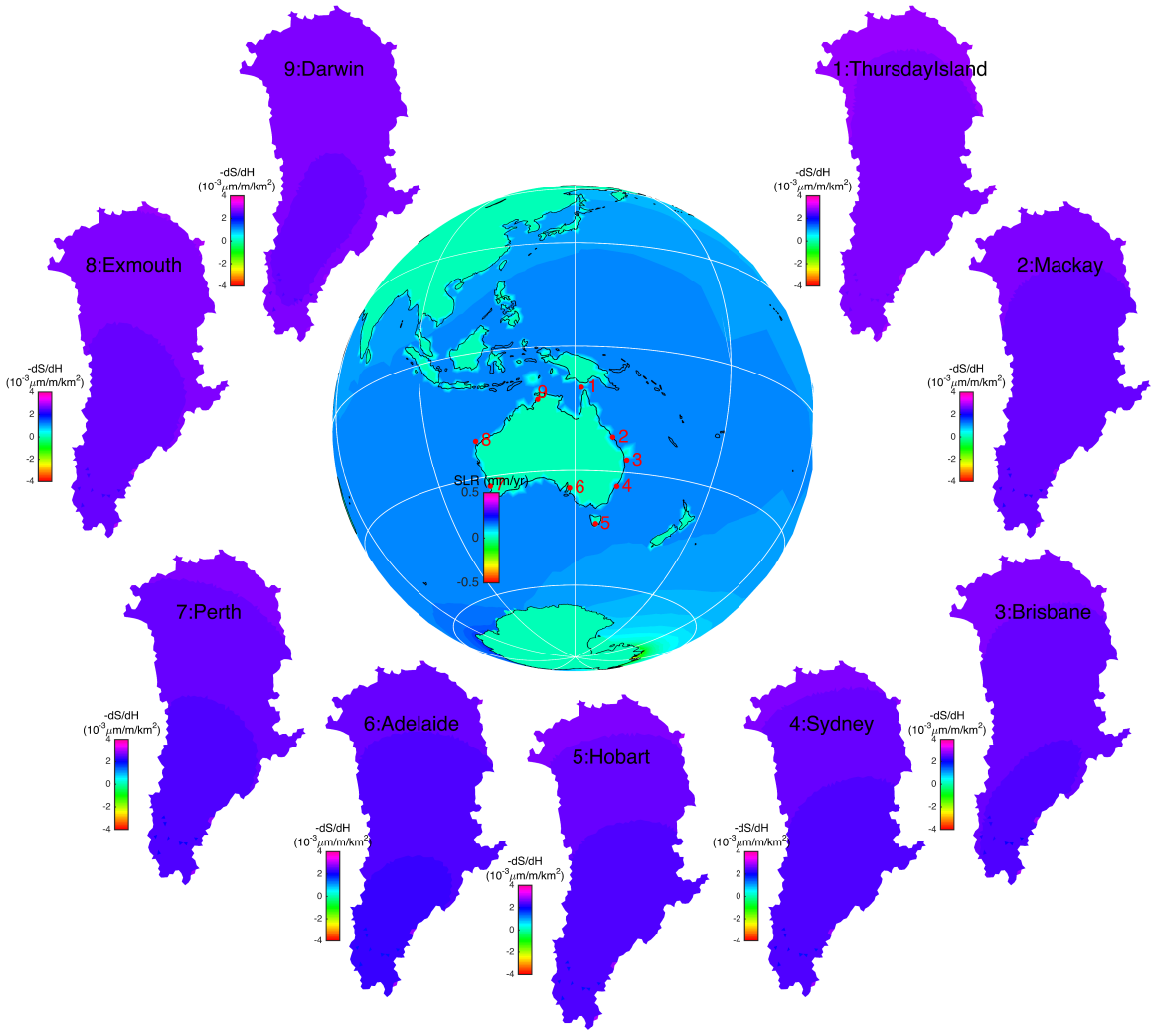

fig. S7. Sensitivity of SLR along the Australian coastline to GrIS thickness variations. Gradient −dS/dH (in μm/m/km^2) at select Australian coastal cities. Maps 1 through 9 correspond, respectively, to gradients computed for each of the named ports numbered clockwise from Thursday Island. See Fig. 2 caption for a detailed explanation of how the forward run and its gradient were computed.

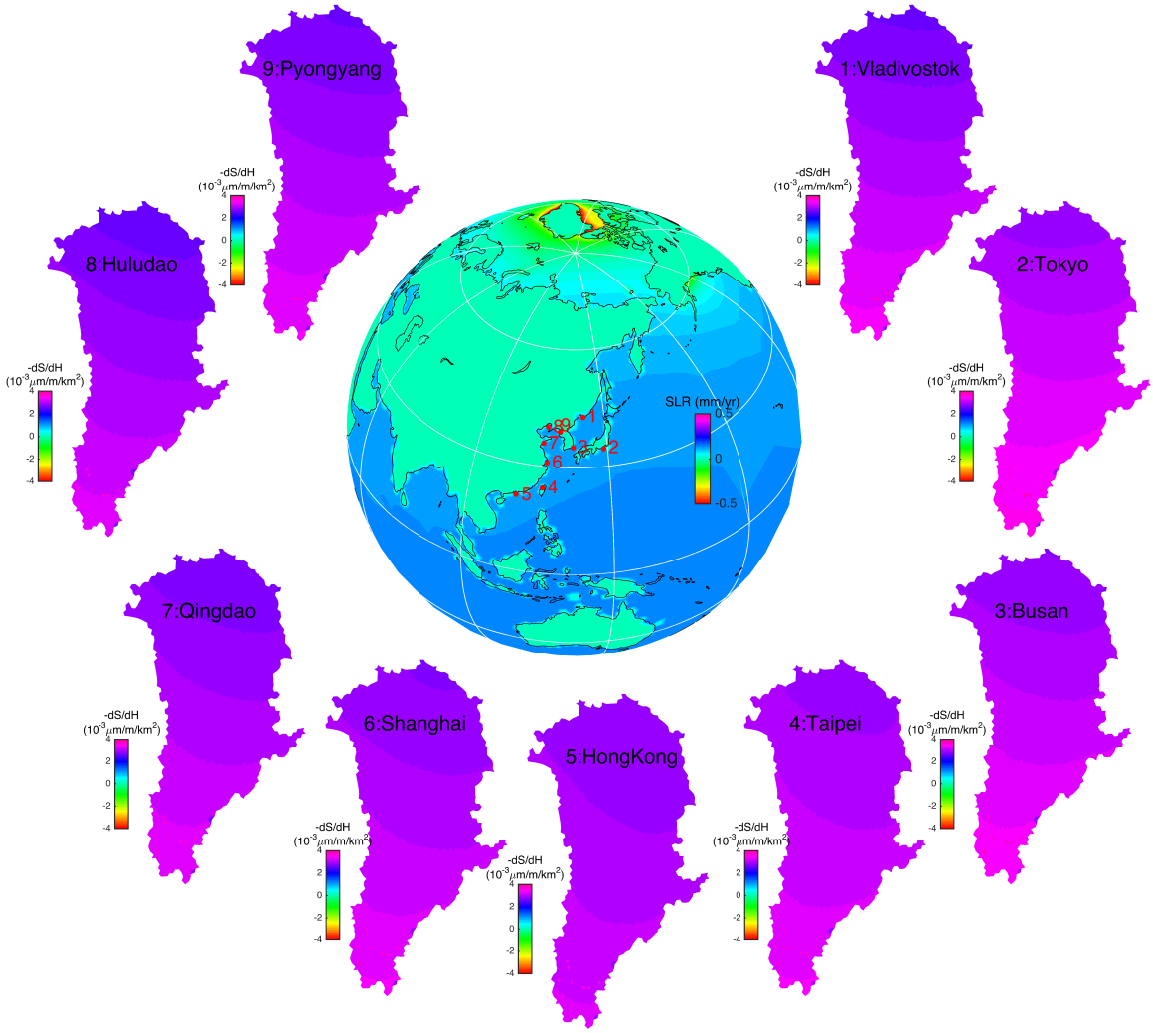

fig. S8. Sensitivity of SLR along the East Asian coastline to GrIS thickness variations. Gradient −dS/dH (in μm/m/km^2) at select East-Asian coastal cities. Maps 1 through 9 correspond, respectively, to gradients computed for each of the named ports numbered clockwise from Vladivostok. See Fig. 2 caption for a detailed explanation of how the forward run and its gradient were computed.

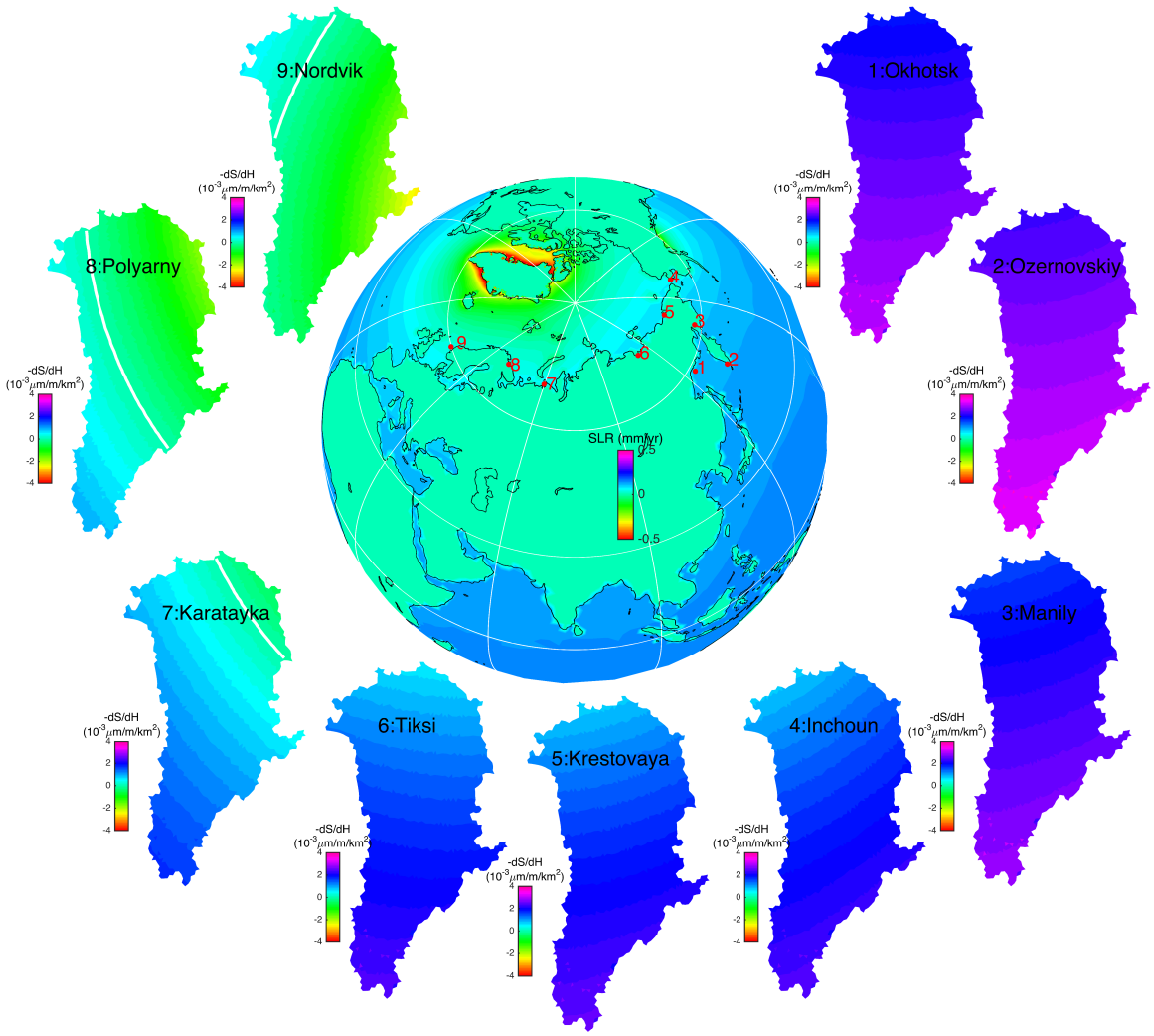

fig. S9. Sensitivity of SLR along the Northeast Asian and the Russian Arctic coastlines to GrIS thickness variations. Gradient −dS/dH (in μm/m/km^2) at select North-East Asian and Russian Arctic coastal cities. Maps 1 through 9 correspond, respectively, to gradients computed for each of the named ports numbered clockwise from Okhotsk. The zero level for the gradient is marked by a white line. See Fig. 2 caption for a detailed explanation of how the forward run and its gradient were computed.

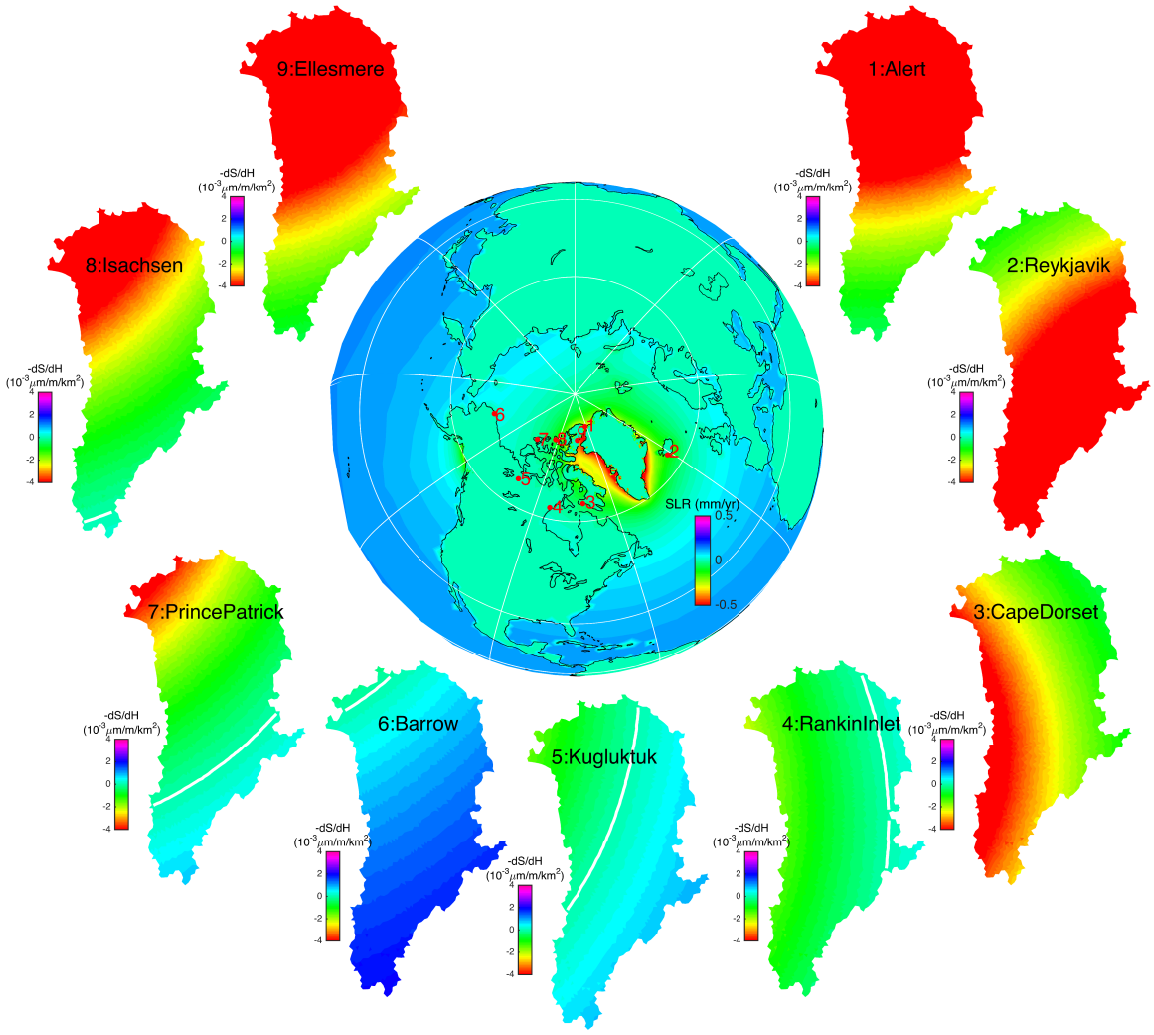

fig. S10. Sensitivity of SLR along the Canadian Arctic coastline to GrIS thickness variations. Gradient −dS/dH (in μm/m/km^2) at select Canadian Arctic coastal cities. Maps 1 through 9 correspond, respectively, to gradients computed for each of the named ports numbered clockwise from Alert. A white line marks the zero level for the gradient. See Fig. 2 caption for a detailed explanation of how the forward run and its gradient were computed.

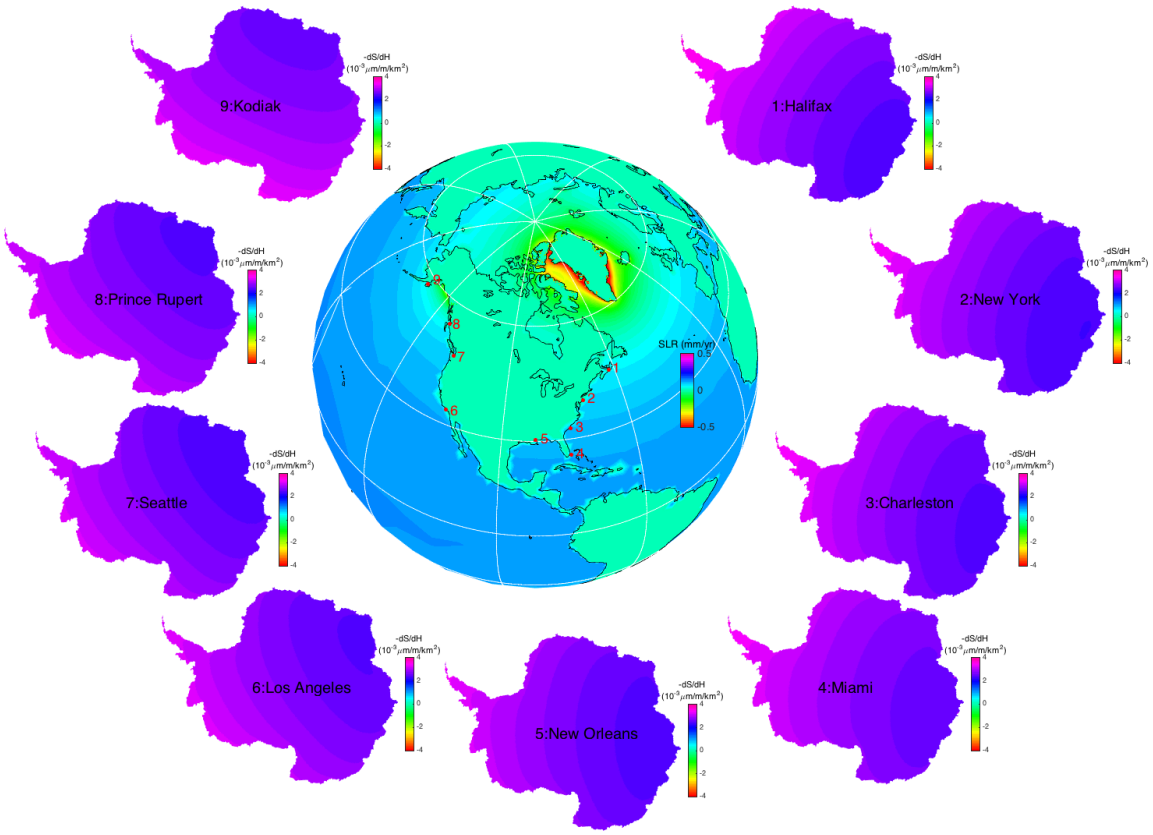

fig. S11. Sensitivity of SLR along the North American coastline to AIS thickness variations. Gradient −dS/dH (in μm/m/km^2) at select North-American coastal cities. Maps 1 through 9 correspond, respectively, to gradients computed for each of the named ports numbered clockwise from Halifax. See Fig. 2 caption for a detailed explanation of how the forward run and its gradient were computed.

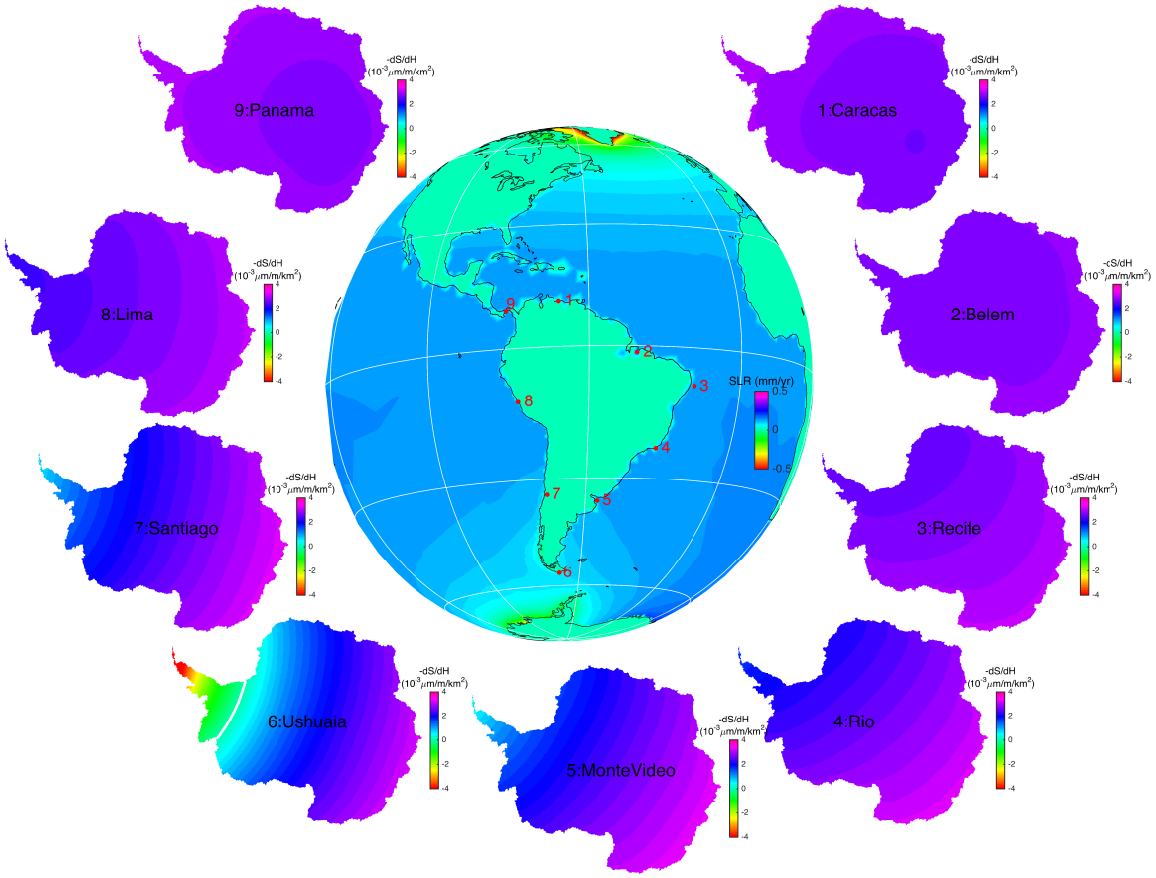

fig. S12. Sensitivity of SLR along the South American coastline to AIS thickness variations. Gradient −dS/dH (in μm/m/km^2) at select South-American coastal cities. Maps 1 through 9 correspond, respectively, to gradients computed for each of the named ports numbered clockwise from Caracas. A white line marks the zero level for the gradient. See Fig. 2 caption for a detailed explanation of how the forward run and its gradient were computed.

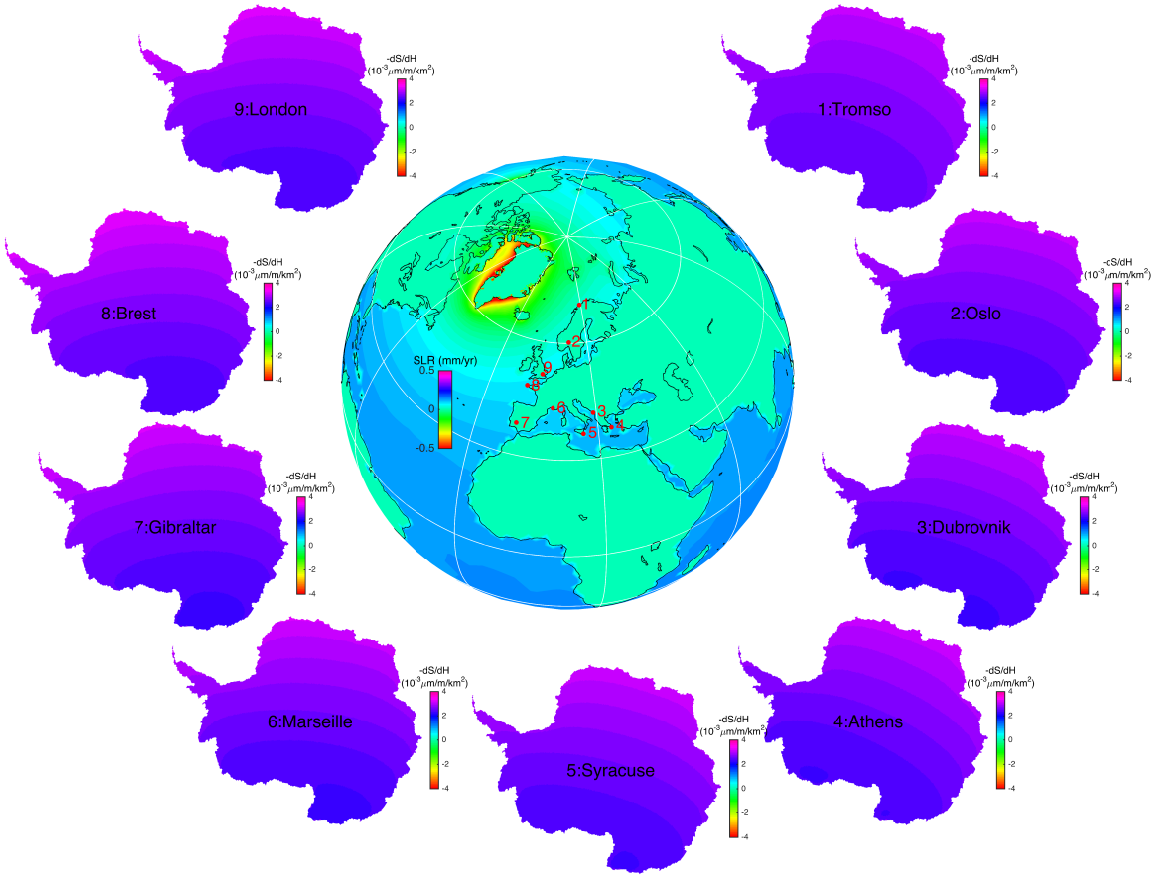

Fig. S13. Sensitivity of SLR along the European coastline to AIS thickness variations. Gradient −dS/dH (in μm/m/km^2) at select European coastal cities. Maps 1 through 9 correspond, respectively, to gradients computed for each of the named ports numbered clockwise from Tromso. See Fig. 2 caption for a detailed explanation of how the forward run and its gradient were computed.

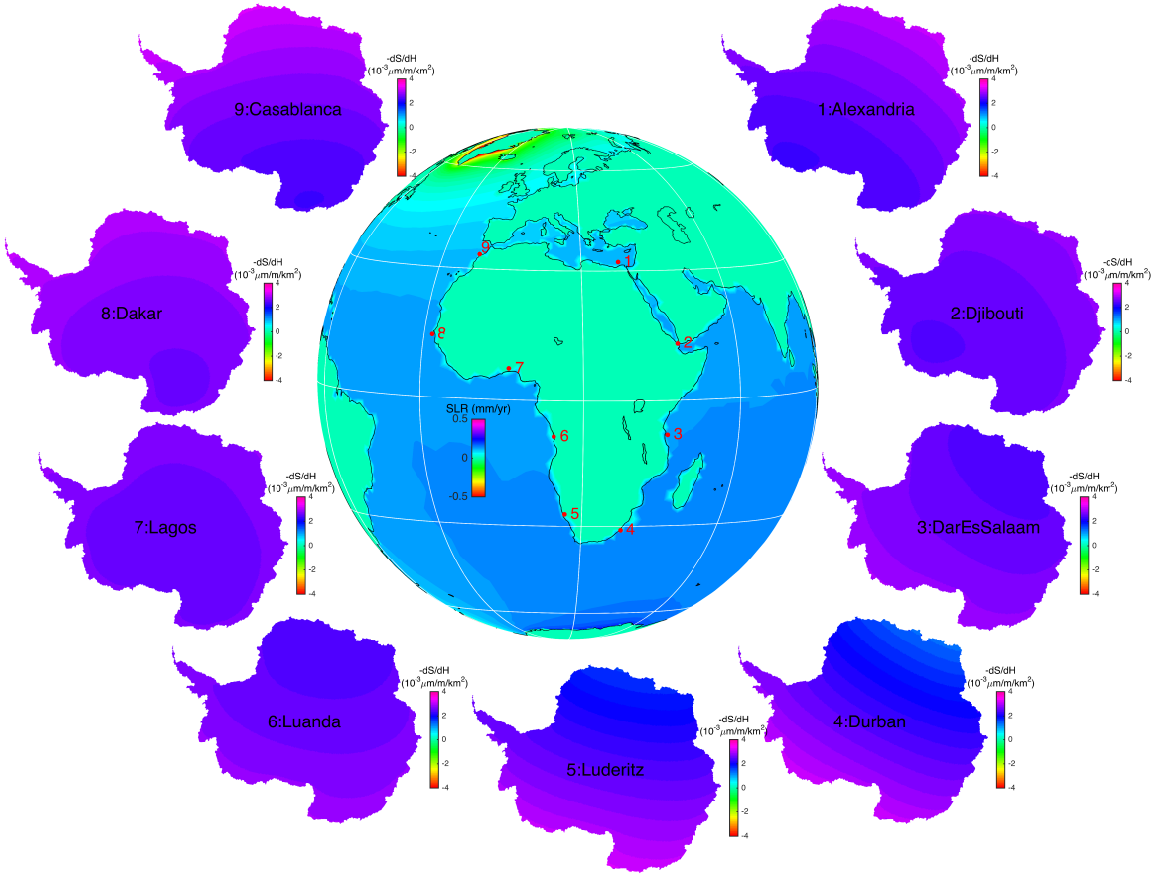

fig. S14. Sensitivity of SLR along the African coastline to AIS thickness variations. Gradient −dS/dH (in μm/m/km^2) at select African coastal cities. Maps 1 through 9 correspond, respectively, to gradients computed for each of the named ports numbered clockwise from Alexandria. See Fig. 2 caption for a detailed explanation of how the forward run and its gradient were computed.

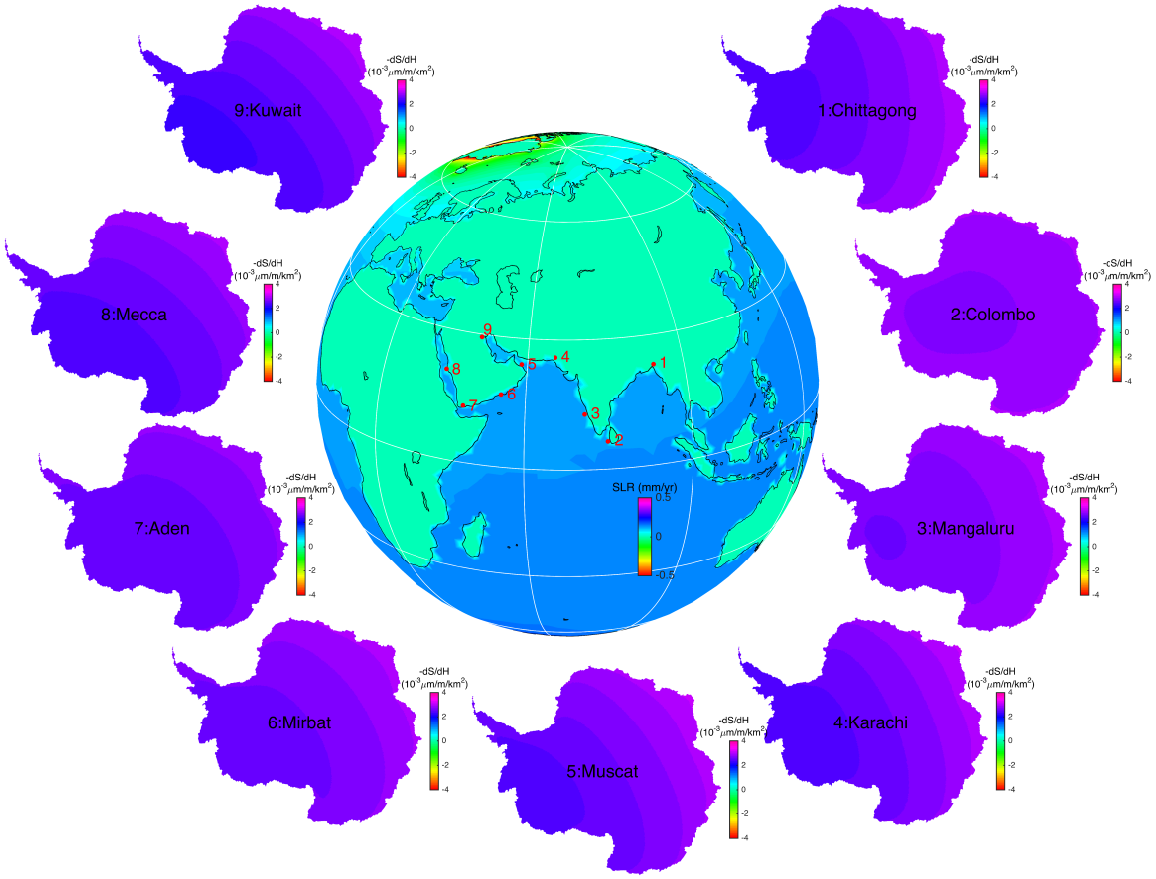

fig. S15. Sensitivity of SLR along Middle East and Southeast Asian coastlines to AIS thickness variations. Gradient −dS/dH (in μm/m/km^2) at select Middle-East and South-East Asian coastal cities. Maps 1 through 9 correspond, respectively, to gradients computed for each of the named ports numbered clockwise from Chittagong. See Fig. 2 caption for a detailed explanation of how the forward run and its gradient were computed.

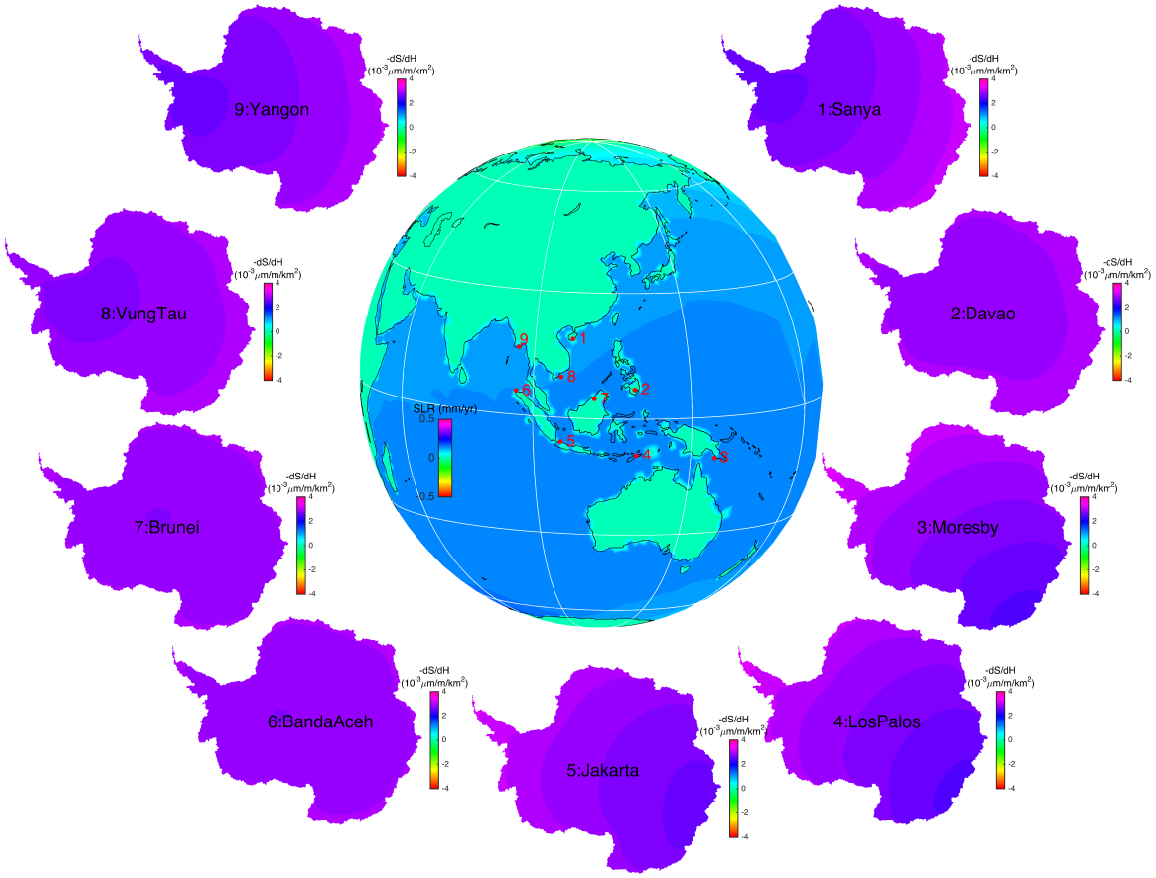

fig. S16. Sensitivity of SLR along the Southeast Asian coastline to AIS thickness variations. Gradient −dS/dH ((in μm/m/km^2) at select South-East Asian coastal cities. Maps 1 through 9 correspond, respectively, to gradients computed for each of the named ports numbered clockwise from Sanya. See Fig. 2 caption for a detailed explanation of how the forward run and its gradient were computed.

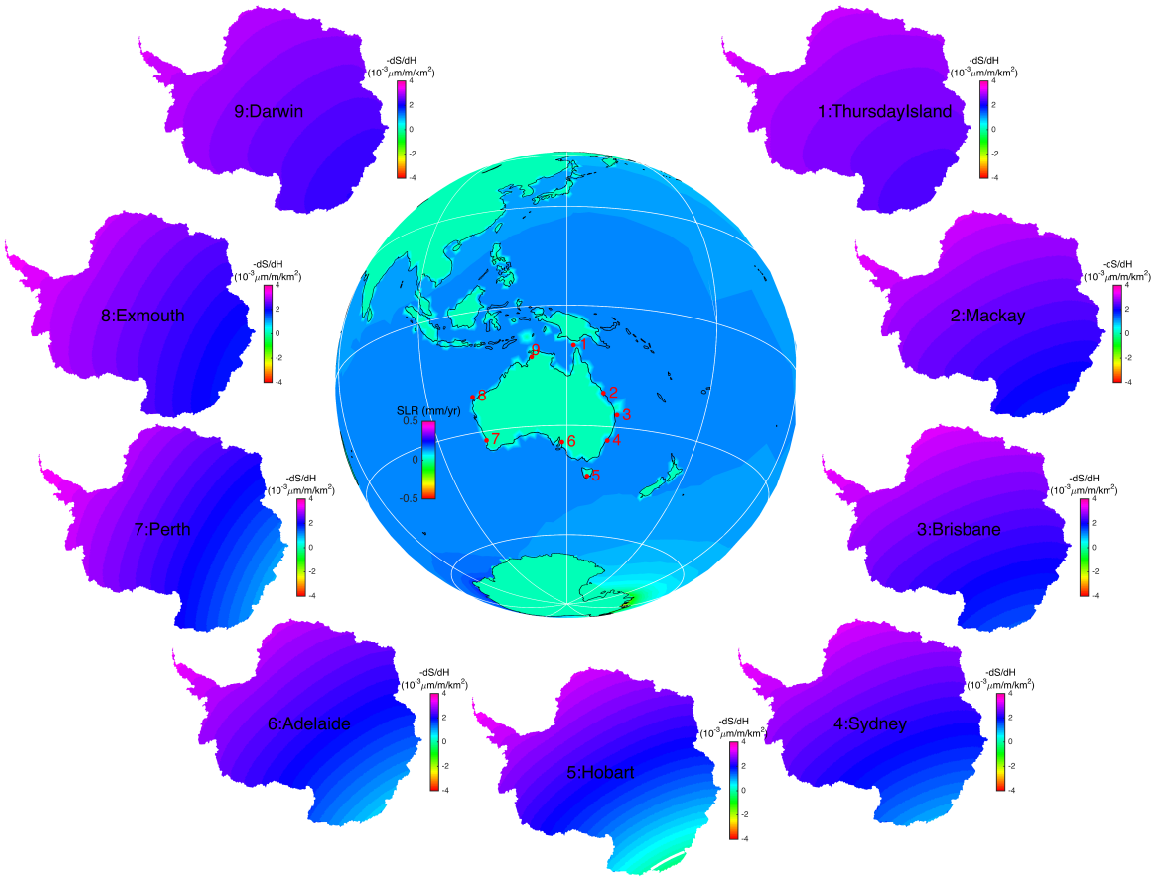

fig. S17. Sensitivity of SLR along the Australian coastline to AIS thickness variations. Gradient −dS/dH (in μm/m/km^2) at select Australian coastal cities. Maps 1 through 9 correspond, respectively, to gradients computed for each of the named ports numbered clockwise from Thursday Island. A white line marks the zero level for the gradient. See Fig. 2 caption for a detailed explanation of how the forward run and its gradient were computed.

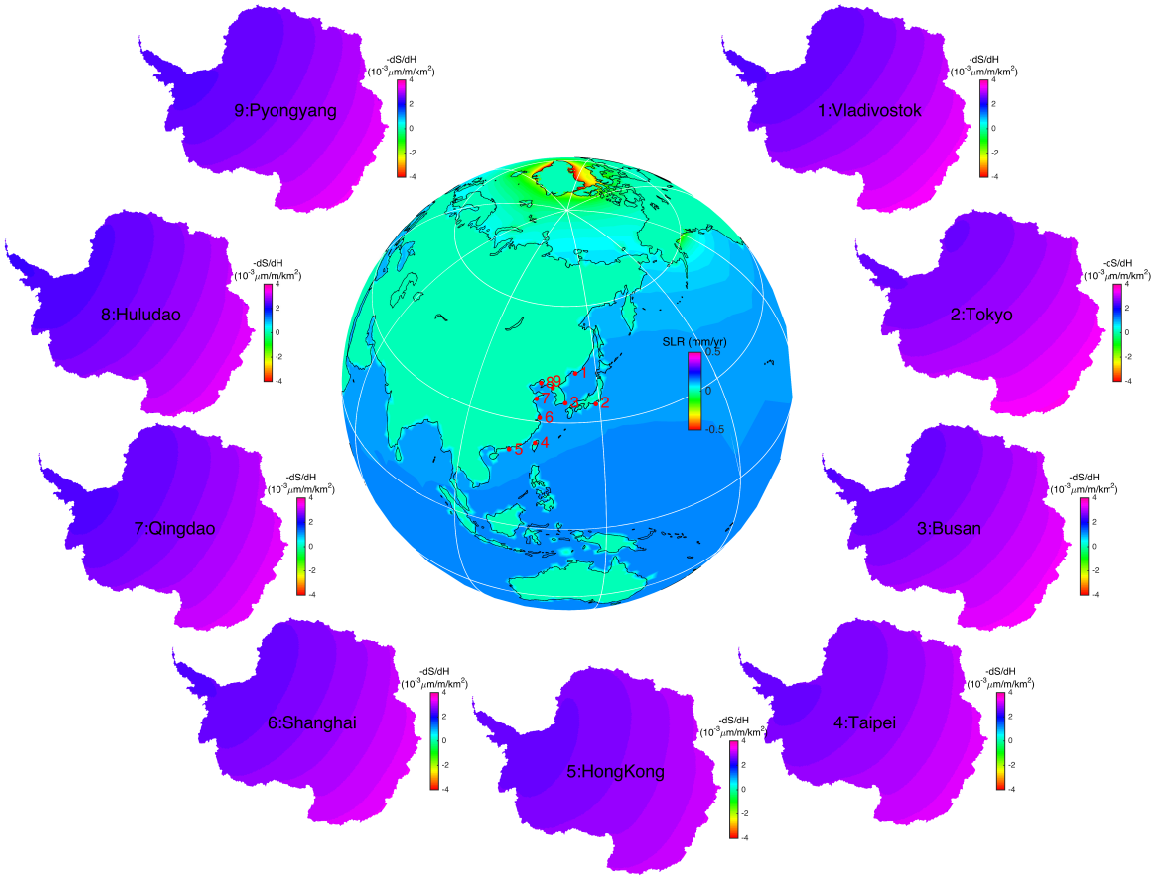

fig. S18. Sensitivity of SLR along the East Asian coastline to AIS thickness variations. Gradient −dS/dH (in μm/m/km^2) at select East-Asian coastal cities. Maps 1 through 9 correspond, respectively, to gradients computed for each of the named ports numbered clockwise from Vladivostok. See Fig. 2 caption for a detailed explanation of how the forward run and its gradient were computed.

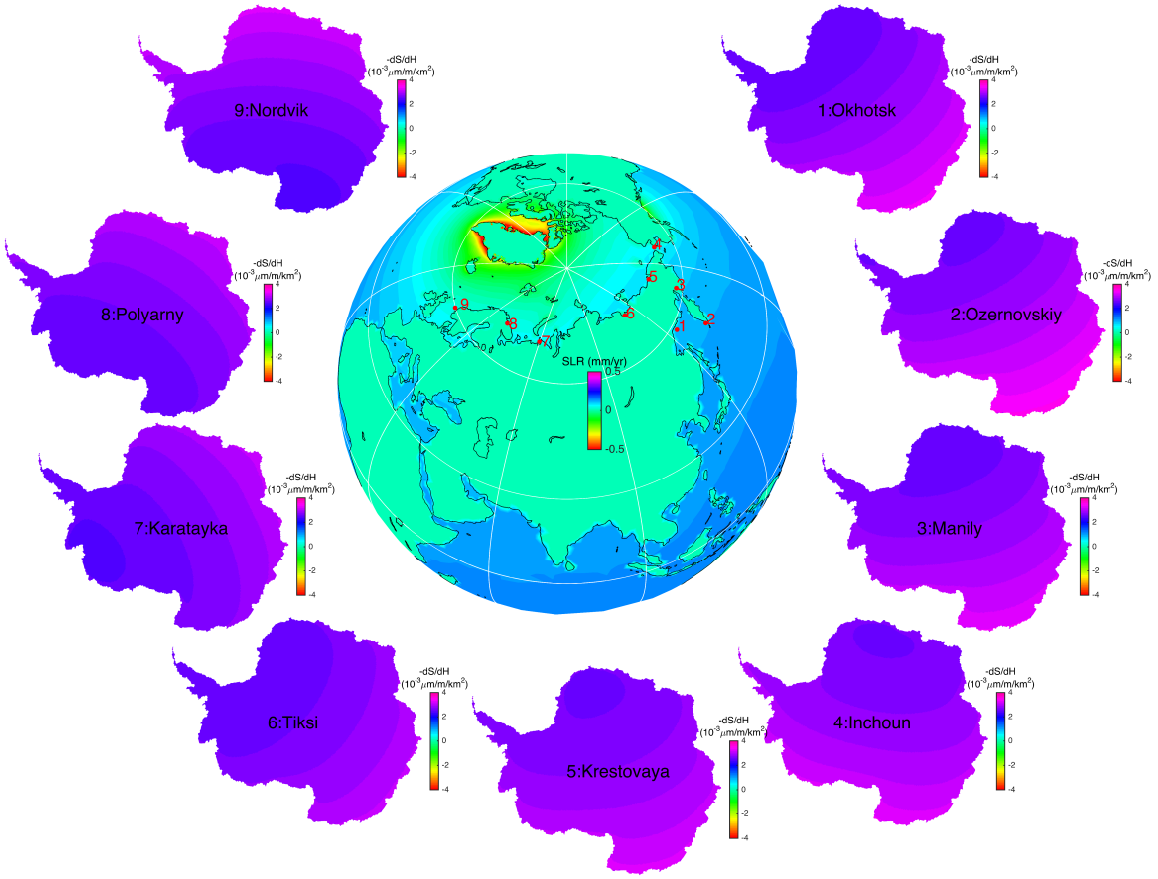

fig. S19. Sensitivity of SLR along the Northeast Asian and the Russian Arctic coastlines to AIS thickness variations. Gradient −dS/dH (in μm/m/km^2) at select North-East Asian and Russian Arctic coastal cities. Maps 1 through 9 correspond, respectively, to gradients computed for each of the named ports numbered clockwise from Okhotsk. See Fig. 2 caption for a detailed explanation of how the forward run and its gradient were computed.

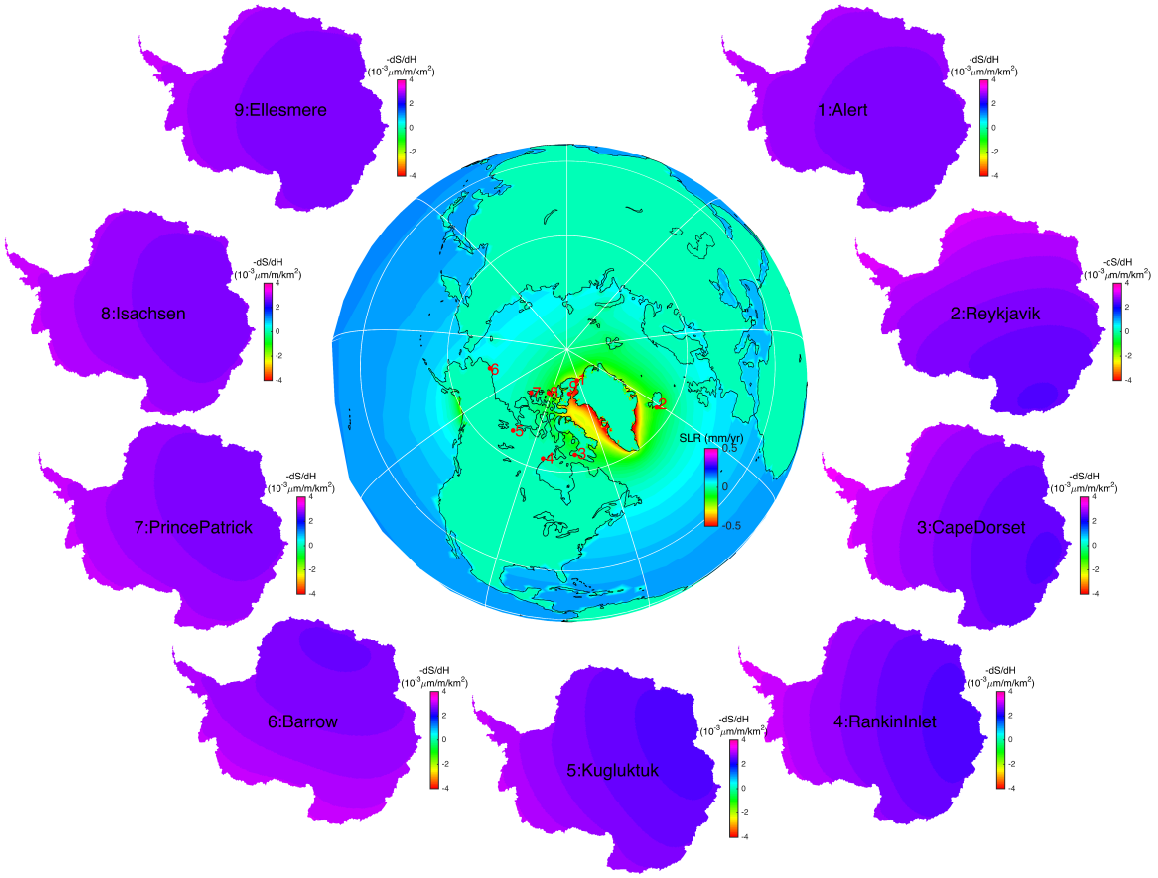

fig. S20. Sensitivity of SLR along the Canadian Arctic coastline to AIS thickness variations. Gradient −dS/dH (in μm/m/km^2) at select Canadian Arctic coastal cities. Maps 1 through 9 correspond, respectively, to gradients computed for each of the named ports numbered clockwise from Alert. See Fig. 2 caption for a detailed explanation of how the forward run and its gradient were computed.

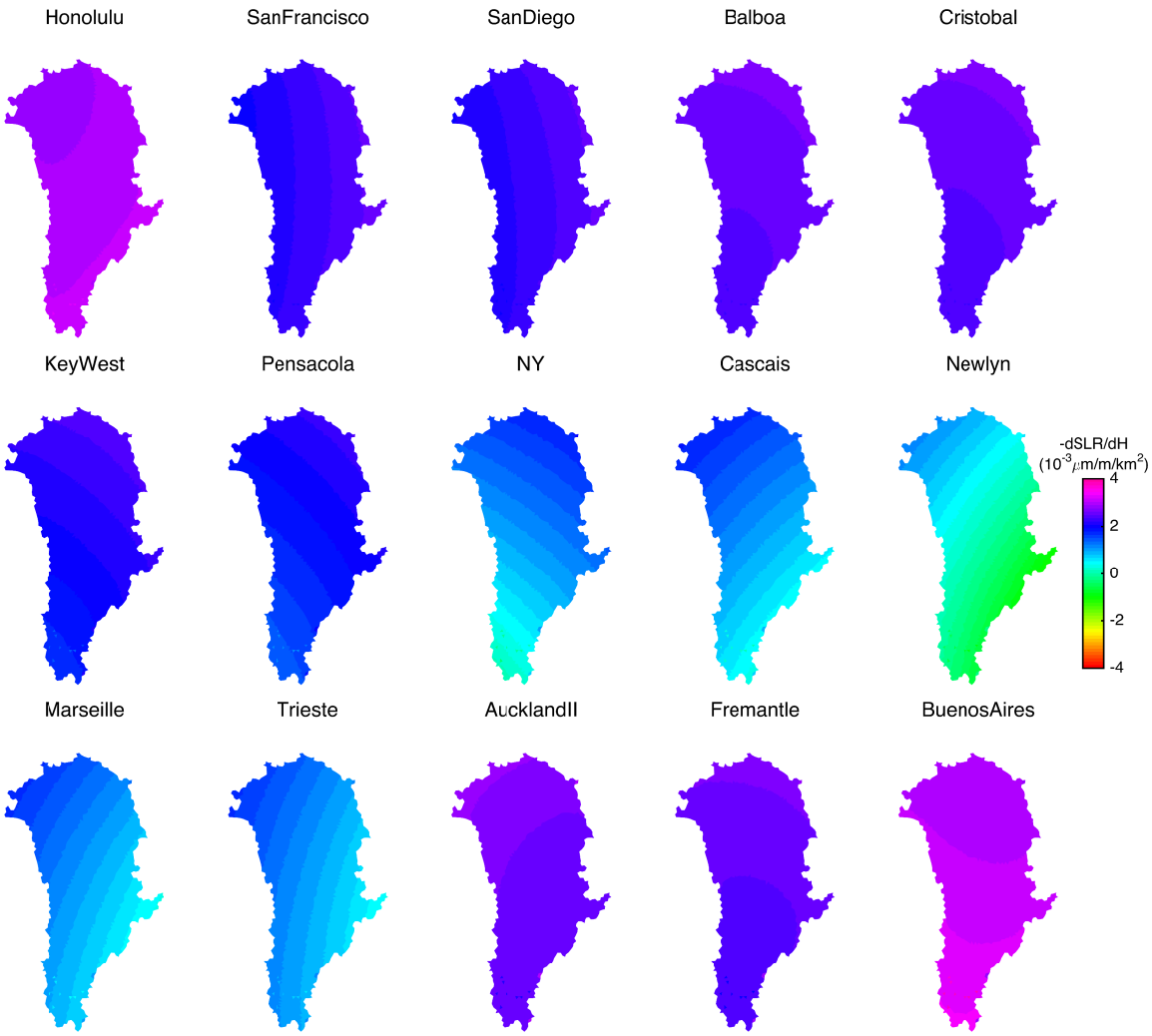

fig. S21. Sensitivity of SLR for 15 reliable tide gauges around the world to GrIS thickness variations. Gradient −dS/dH (in μm/m/km^2) in Greenland for the 15 tide gauges defined in (32). See Fig. 2 caption for a detailed explanation of how the forward run and its gradient were computed.

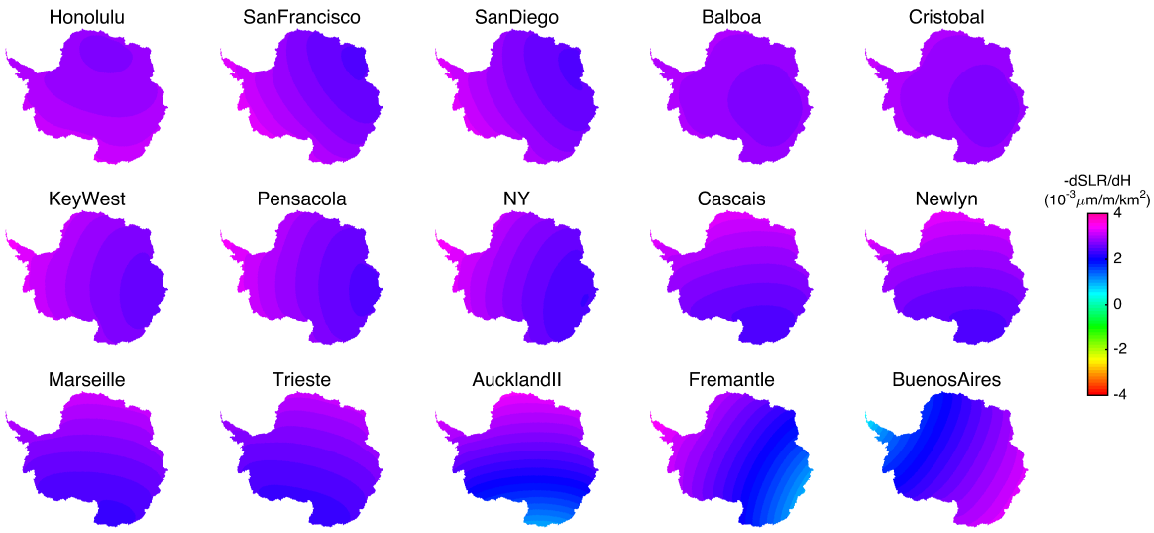

fig. S22. Sensitivity of SLR for 15 reliable tide gauges around the world to AIS thickness variations. Gradient −dS/dH (in μm/m/km^2) in Antarctica for the 15 tide gauges defined in (32). See Fig. 2 caption for a detailed explanation of how the forward run and its gradient were computed.